EEET ECOLOGICAL ENGINEERING & ENVIRONMENTAL TECHNOLOGY

Ecological Engineering & Environmental Technology, 2026, 27(9), 92–109
https://doi.org/10.12912/27197050/226089
ISSN 2719–7050, License CC-BY 4.0

Received: 2026.07.07
Accepted: 2026.07.30
Published: 2026.08.15

Flood vulnerability assessment in the Oued Bounouara Watershed (northeastern Algeria) using remote sensing, GIS, and AHP-based multi-criteria analysis

Benoudina Nouha Amira[1*], Djeghar Aïda[1], Taibi Ibrahim El Khalil[2], Grecu Florina[3], Benchenna Abdelali[4]

[1] BIOSTIM Laboratory, Institute GTU, Department of Urban Management Techniques and Environment, University of Constantine 3 Salah Boubnider, Ali Mendjeli University Campus, New City, Constantine, Algeria
[2] Geography and Regional Planning Laboratory (LGAR), Higher Normal School of Teachers ENSL – Taleb Abderrahman, Algeria
[3] Department of Geomorphology, Pedology, and Geomatics, Faculty of Geography, University of Bucharest, 1 N. Bălcescu Boulevard, Sector 1, Bucharest, Romania
[4] Department of Architecture, Faculty of Sciences and Technology, University of Jijel, 18000 Jijel, Algeria
* Corresponding author's e-mail: nouha.benoudina@univ-constantine3.dz

ABSTRACT

Floods are among the most destructive natural hazards affecting Mediterranean watersheds, causing significant environmental, economic, and social impacts. This study aims to assess flood vulnerability in the Oued Bounouara Watershed (northeastern Algeria) by integrating geographic information systems (GIS) and the analytical hierarchy process (AHP). Seven flood-conditioning factors, namely altitude, slope, precipitation, land use, lithology, stream proximity, and flow accumulation, were weighted using the AHP method and integrated through a GIS-based weighted overlay approach to produce a flood vulnerability map. The resulting map classified the watershed into five vulnerability classes and revealed that approximately 34% of the study area falls within the high and very high vulnerability categories, mainly concentrated in the western sector and along the main hydrographic network. The predictive performance of the model was evaluated using an independent validation database consisting of 360 reference points, including 180 documented flood occurrence points and 180 non-flood points compiled from civil protection records, municipal archives, historical reports, previous technical documents, and field investigations. Validation results demonstrated that the proposed GIS–AHP model achieved good predictive capability, with 100% of the documented flood occurrences located within the high and very high vulnerability classes. The success rate curve (SRC) analysis produced an area under the curve (AUC) value of 0.795, indicating good predictive performance, while the success curve area ratio (SCAR = 2.94) confirmed a strong concentration of flood occurrences within highly vulnerable areas. Sensitivity analysis further demonstrated the robustness of the model under moderate variations in the thematic weights. The proposed GIS–AHP framework provides a reliable, transparent, and transferable approach for flood vulnerability assessment and represents an effective decision-support tool for land-use planning, flood mitigation, infrastructure management, and disaster risk reduction in Mediterranean watersheds and other data-scarce regions.

Keywords: flood, risk, AHP, Bounouara Watershed, GIS, remote sensing, vulnerability, Constantine.

INTRODUCTION

Floods are among the most frequent and destructive natural hazards worldwide, causing substantial environmental degradation, economic losses, infrastructure damage, and loss of human life. In recent decades, climate change has significantly altered global precipitation regimes, increasing both the frequency and intensity of extreme rainfall events and consequently exacerbating flood hazards in many regions (Reidy, 2016). Since the 1950s, global warming has contributed to more frequent extreme weather events, with scientific projections indicating that extreme precipitation may increase by approximately 7% for every 1 °C rise in global temperature (Ziadi and Keraghel, 2024). These climatic changes have transformed flood risk into one of the most critical environmental challenges facing both developed and developing countries (Uca et al., 2022).

Flood vulnerability is controlled by a complex interaction between natural environmental conditions and anthropogenic activities. Topography, geology, rainfall distribution, drainage characteristics, and land cover govern runoff generation and flood propagation, while rapid urbanization, population growth, and inadequate land-use planning considerably increase the exposure and vulnerability of communities (Grecu, 2018). This situation is particularly critical in developing countries, where urban expansion often occurs without adequate flood management infrastructure or effective spatial planning. Consequently, accurate flood vulnerability assessment has become an essential component of sustainable watershed management and disaster risk reduction.

Africa represents one of the regions most vulnerable to flood hazards because of the combined effects of climate change, rapid urban growth, insufficient drainage infrastructure, and increasing demographic pressure (Boukhiar et al., 2024; Angie, 2025). Sub-Saharan African countries experience some of the highest flood-related mortality rates worldwide, with informal settlements generally occupying the most flood-prone areas. Globally, floods account for more than 80% of all natural disasters and affect over 230 million people annually, generating average economic losses exceeding USD 120 billion each year (Germanwatch, 2024). Beyond their economic consequences, floods remain the second deadliest natural hazard after drought, causing approximately 18,000 fatalities every year.

Algeria is no exception to this increasing flood risk. During the last two decades, the country has experienced several catastrophic flood events, including the Bab El Oued disaster in 2001, which resulted in more than 335 fatalities, the Djanet floods in 2005, the Ghardaïa floods in 2008, the Djelfa floods in 2015, and the more recent flood events affecting Béchar in 2024 (Bourenane and Bouhadad, 2020; Kalla, 2024). In northeastern Algeria, the Wilaya of Constantine has also experienced recurrent flooding between 2018 and 2024, causing extensive damage to infrastructure, agricultural land, and residential areas (Rebouh et al., 2024). The continuous expansion of urban areas into natural floodplains, combined with insufficient drainage systems and uncontrolled land-use changes, has significantly increased flood vulnerability throughout the region (Djedaiet et al., 2024).

Among the watersheds exposed to recurrent flooding in northeastern Algeria, the Oued Bounouara watershed represents one of the most vulnerable areas. Major flood events have been documented in March 2011, August 2013, April 2017, May 2023, and September 2024 (Aktar et al., 2021). One remarkable event occurred in Ain Abid, where an intense rainfall episode lasting only 40 minutes caused the water level of Oued Bounouara to rise from approximately 40 cm to 70 cm, illustrating the flash-flood behavior that characterizes Mediterranean watersheds. These recurrent flood events have repeatedly affected residential neighborhoods, transportation infrastructure, and agricultural lands, demonstrating the increasing vulnerability of local communities.

The Oued Bounouara watershed covers approximately 181 km^2 and constitutes an important tributary of the Boumerzoug watershed in the Constantine region. Its hydrological behavior is strongly influenced by steep topography, heterogeneous lithological formations, and a well-developed dendritic drainage network that rapidly concentrates runoff during high-intensity rainfall events. Recent hydraulic simulations using HEC-RAS further confirmed the high flood potential of the watershed, with simulated flood depths exceeding 7 m in the most vulnerable sectors (Benoudina et al., 2026). These physical characteristics, combined with the rapid expansion of peri-urban settlements, considerably increase both flood occurrence and human exposure.

Recognizing the growing impacts of flood disasters, local authorities have increasingly emphasized the need to integrate flood risk assessment into territorial planning and infrastructure development. Following the devastating floods of May 2023, the authorities of Constantine highlighted the urgent necessity of implementing proactive flood prevention strategies and improving watershed management practices. Consequently, reliable flood vulnerability mapping has become an essential decision-support tool for guiding land-use planning, infrastructure development, emergency preparedness, and disaster risk reduction.

Advanced geospatial technologies have substantially improved flood vulnerability assessment during the last two decades. GIS, remote sensing, multi-criteria decision analysis (MCDA), and machine-learning techniques are now widely employed to evaluate flood-prone areas and support flood risk management (Samanta et al., 2018). Among these approaches, the integration of GIS with the analytical hierarchy process (AHP) has become one of the most widely adopted methodologies because it combines the spatial analytical capabilities of GIS with a systematic procedure for weighting flood-conditioning factors (Kazakis et al., 2015). More recently, hybrid approaches integrating GIS with machine-learning algorithms have further improved predictive performance in flood susceptibility studies (Pham et al., 2020; Naghibi et al., 2020).

Despite these technological advances, flood vulnerability assessment in Algerian watersheds remains relatively limited, particularly at the scale of small and medium-sized peri-urban catchments. Most existing studies have focused on large metropolitan areas or major river systems, whereas smaller watersheds experiencing rapid urban expansion and recurrent flooding have received comparatively little scientific attention (Guellouh et al., 2023). Consequently, the complex interactions between watershed morphometry, land-use dynamics, climatic variability, and increasing human exposure remain insufficiently documented in these environments. This knowledge gap is particularly important because peri-urban watersheds often experience rapid and unplanned urban development while lacking the hydraulic infrastructure and flood mitigation capacity commonly available in larger cities.

The Oued Bounouara Watershed represents a particularly relevant case study in this context. Over the last decade, the watershed has experienced several damaging flood events that have affected residential areas, transportation networks, and agricultural lands. At the same time, continuous urban expansion has progressively increased the exposure of the local population to flood hazards. Despite its socio-economic importance and recurrent flood history, no comprehensive GIS-based flood vulnerability assessment has previously been conducted for this watershed. Therefore, developing a reliable flood vulnerability map is essential for supporting land-use planning, infrastructure development, emergency preparedness, and long-term flood risk reduction.

The primary objective of this study is to develop a flood vulnerability map for the Oued Bounouara Watershed by integrating GIS with the AHP. Seven flood-conditioning factors elevation, slope, precipitation, land use, lithology, flow accumulation, and stream proximity were selected based on previous literature and the physical characteristics of the watershed. These factors were standardized, weighted using the AHP approach, and integrated through a GIS-based weighted overlay analysis to produce the final flood vulnerability map.

Although the GIS–AHP methodology employed in this study is well established, the scientific contribution of this research lies in its application to a previously unstudied Mediterranean peri-urban watershed characterized by recurrent flood events, rapid urban expansion, and increasing socio-environmental vulnerability. Unlike most previous flood vulnerability studies conducted in Algeria, which primarily focus on large urban centers, this research investigates a smaller watershed where natural hydrological processes interact directly with peri-urban development, creating highly dynamic flood-risk conditions. Furthermore, the study integrates official governmental datasets, remotely sensed information, and field observations within a transparent and reproducible GIS framework. The resulting flood vulnerability model is independently validated using a balanced reference database consisting of 180 documented flood occurrence points and 180 non-flood points, thereby enhancing the robustness and credibility of the assessment. Beyond supporting local flood risk management, the proposed framework provides a transferable methodology for flood vulnerability assessment in other Mediterranean watersheds facing similar environmental conditions and limited data availability (Figure 1).

STUDY AREA

The Wilaya of Constantine faces significant hydrological challenges (Yakhlefoune, et al., 2023), particularly within its sub-basins, including the Boumerzoug region, which serves as the focal point of this study.

The research specifically examines the Bounouara region, located on the southeastern periphery of Constantine, known as the "City of Bridges".

Situated in northeastern Algeria at coordinates 36°18′N, 6°37′E, at an elevation ranging from 640 to 86 m above sea level (Oussalah et al., 2023).

Figure 1. Floods of 4 May 2023, the municipality of Ouled Rahmoun

The region experiences a Mediterranean climate with semi-arid characteristics, characterized by hot, dry summers and mild, wet winters, with annual precipitation ranging from 600 to 800 mm.

The study area encompasses two municipalities: Ouled Rahmoun, which includes the Bounouara agglomeration, and Ain Abid, home to the Kehalcha-Kebar agglomeration. Both municipalities are highly susceptible to hydrological risks.

Ouled Rahmoun municipality covers approximately 85 km² and has a population of 45,000 inhabitants (INS, 2024) Ain Abid, located 15 km southeast of Constantine, covers 120 km² with a population of 68,000, experiencing rapid urbanization at a rate of 3.2% annually. This rapid population growth, combined with unregulated urban expansion, has significantly increased exposure to flood hazards in both municipalities.

Watershed characteristics

The Oued Bounouara Watershed is located in the northeastern part of the Oued Boumerzoug basin (hydrological code 10-05), as defined by the National Agency of Hydraulic Resources (ANRH). It is drained by the Oued Bounouara, which originates in Chaabet El Bey near Bled Mhiriss, flows northward before turning westward, and eventually joins Oued Berda. The watershed covers an area of 181 km², with a perimeter of 64 km and a main channel length of 24 km. Its drainage density is 1.33 km km^{-2}, indicating a moderately developed drainage network typical of Mediterranean watersheds with heterogeneous lithological conditions (Chen et al., 2019).

Morphometric analysis indicates that the watershed has an elongated geometry. The Gravelius coefficient of 1.33 and the elongation coefficient of 3.18 confirm a moderate departure from a circular shape. The equivalent rectangular dimensions are 22.21 km in length and 9.58 km in width. Such an elongated morphology generally increases the time of concentration and tends to attenuate peak discharges; however, this effect is partially offset by the steep relief that characterizes the northern part of the watershed (Meroti et al., 2020).

The watershed exhibits considerable topographic variability, with elevations ranging from 680 m to 1.294 m above sea level, corresponding to a mean elevation of 888.86 m and a total relief of 614 m. This pronounced altitudinal gradient provides substantial gravitational energy for surface runoff, promoting rapid flow concentration from the mountainous upstream areas toward the downstream valleys (Tehrany et al., 2019; Arabameri et al., 2021).

Terrain slopes vary markedly throughout the watershed. The southern sector is characterized by relatively gentle slopes (<15%), whereas the northern highlands commonly exhibit gradients between 30% and 50%, locally exceeding 50%. The mean watershed slope is approximately 28%, indicating rugged topography that strongly favors rapid runoff generation, reduced infiltration, and flash flood development during intense rainfall events (Tremlett et al., 2021).

The drainage network displays a well-developed dendritic pattern, reflecting relatively homogeneous geological control and limited structural influence on channel development. According to the Strahler stream-order classification, the main watercourse is classified as a fourth-order stream, supplied by numerous first- and second-order tributaries (Grecu, 2017). This hierarchical drainage structure efficiently concentrates runoff from upstream sub-catchments and accelerates flood wave propagation during heavy rainfall.

The watershed is crossed by National Road No. 20, which constitutes one of the principal transportation corridors connecting Constantine with the southeastern part of the province. This infrastructure, together with the continuous expansion of urban areas within the watershed, increases exposure to flood hazards by placing residential areas, transportation networks, and public facilities within flood-prone zones.

The Oued Bounouara Watershed has experienced several significant flood events during the last two decades, notably in 2011, 2013, 2017, 2023, and 2024 (Aktar et al., 2021). These recurrent floods have caused considerable damage to infrastructure, agricultural land, and residential areas, confirming the high hydrological sensitivity of the watershed. The combination of steep topography, elongated morphology, efficient drainage organization, and increasing anthropogenic pressure makes the Oued Bounouara watershed particularly susceptible to flash flooding and therefore an appropriate case study for flood vulnerability assessment in Mediterranean environments (Figure 2).

SPATIAL DATABASE AND DATA QUALITY ASSESSMENT

The flood vulnerability assessment was developed using a comprehensive multi-source geospatial database integrating topographic, geological, hydrological, climatic, land-use, and historical flood inventory datasets. The reliability of the analysis largely depends on the quality of the input data; therefore, only official governmental datasets and internationally recognized geospatial products were selected. These datasets were evaluated according to their source, spatial resolution, positional accuracy, temporal relevance, and suitability for watershed-scale flood vulnerability analysis (Table 1).

The primary dataset used in this study is a high-resolution DEM with a spatial resolution of 10 m, derived from the digitization of 1:50,000 topographic maps provided by the National Institute of Geographic Information (Paris 12). Produced in 2015, this DEM provides sufficient topographic detail for hydrological analysis within the Oued Bounouara watershed (181 km²) and served as the basis for generating four essential morphometric and hydrological factors: altitude, slope, flow accumulation, and stream proximity. These thematic layers were generated using the ArcGIS 10.8 Spatial Analyst and Hydrology toolsets, ensuring methodological consistency and minimizing processing errors.

Lithological information was obtained from the National Office for Rural Development (BNEDER) using an official administrative geological map at a scale of 1:50,000. Although this document is not publicly available, it represents the official geological reference used by the institution for land and environmental management. The map provides detailed information on the spatial distribution of the principal geological formations within the watershed, including clayey sandstones, limestone-clay formations, and marls, making it a reliable source for evaluating the influence of lithology on flood vulnerability.

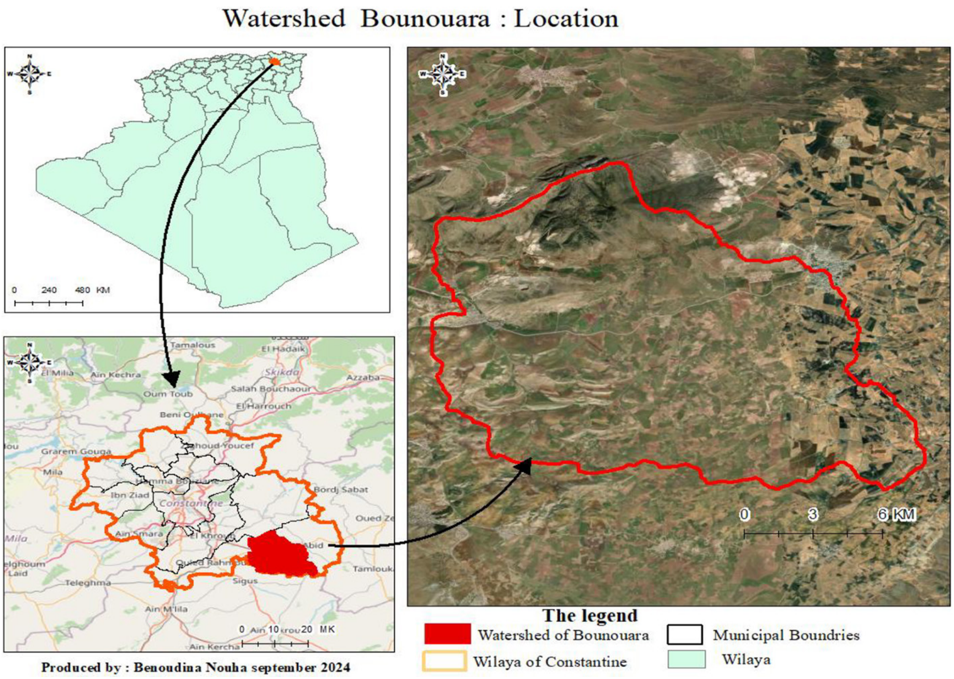

Figure 2. Study area map

Land-use information was derived from Landsat 8 operational land imager (OLI) multispectral imagery with a spatial resolution of 30 m, acquired in 2025 from the USGS EarthExplorer platform. Landsat imagery is radiometrically and geometrically corrected before distribution and has been extensively used worldwide for land-use and land-cover mapping. Its spatial resolution is appropriate for watershed-scale environmental studies and provides consistent information on surface characteristics influencing runoff generation.

Precipitation data were compiled from thirteen meteorological stations distributed across and around the study area using rainfall records collected in 2025 and complemented with the WorldClim Version 2.1 climate database. The combination of local meteorological observations and globally validated interpolated climatic surfaces improves the spatial representation of rainfall variability and enhances the reliability of the precipitation layer.

The historical flood inventory was established by integrating official records provided by the Civil Protection Authority, municipal archives, historical flood reports, previous technical documents, and extensive field investigations conducted throughout the watershed. The final validation database consists of 360 reference points, including 180 confirmed flood occurrence points and 180 non-flood points. The flood occurrence points represent documented flood events recorded between 2011 and 2024 and were verified through field observations, whereas the non-flood points were randomly generated in areas with no documented history of flooding and subsequently checked using field observations and high-resolution satellite imagery. River channels, floodplains, and areas surrounding documented flood locations were excluded from the selection of non-flood points to minimize classification uncertainty and spatial bias. This balanced validation dataset provides a robust and reliable basis for evaluating the predictive performance of the GIS–AHP flood vulnerability model.

Overall, the integration of high-resolution topographic data, official geological information, globally recognized satellite imagery, validated climatic datasets, and field-verified historical flood records ensures a high-quality geospatial database. The complementary nature of these datasets enhances the completeness, consistency, and reliability of the input information, thereby increasing the robustness and credibility of the flood vulnerability assessment performed for the Oued Bounouara watershed.

The metadata associated with each dataset, including the data source, acquisition year, spatial resolution, data format, processing workflow, and quality assessment, are summarized in Table 1. These metadata ensure the traceability, transparency, and reproducibility of the proposed GIS–AHP flood vulnerability assessment. The derived thematic layers (altitude, slope, flow accumulation, and stream proximity) were generated from the 10 m Digital Elevation Model using standard ArcGIS geoprocessing tools, whereas the remaining datasets were obtained from official governmental institutions and internationally recognized geospatial databases.

Historical flood inventory database

To evaluate the predictive performance of the GIS–AHP flood vulnerability model, a historical flood inventory database was developed for the Oued Bounouara watershed. The inventory comprises 180 flood occurrence points and 180 non-flood points, providing a balanced reference dataset for model validation. The spatial distribution of the flood occurrence and non-flood points is presented in Figure 3.

The flood inventory was established by integrating several complementary sources of information. The primary source consisted of official flood records provided by the Civil Protection Directorate of Constantine, which document the locations affected during past flood events. These records were complemented by municipal archives, historical flood reports, previous technical documents, and field investigations carried out throughout the watershed. The inventory covers the principal flood events recorded between 2011 and 2024, including those of March 2011, August 2013, April 2017, May 2023, and September 2024. Since each flood event generally affected several locations, every documented inundated site was georeferenced individually, resulting in a database of 180 flood occurrence points distributed across the watershed. As shown in Figure 3, these flood occurrence points are mainly concentrated along the main river channel and floodplain, whereas the non-flood points are distributed throughout the remaining watershed to represent areas with no documented history of flooding.

To improve the reliability of the inventory, field investigations were conducted at the

Table 1. Metadata and quality assessment of the datasets used

Dataset	Description	Source	Format	Spatial resolution/ Scale	Year	Processing	Reliability
Digital elevation model (DEM)	Digital elevation model derived from digitized topographic maps	National Institute of Geographic Information (Paris 12)	Raster	10 m; 1:50,000	2015	Used as the primary dataset for terrain analysis	Official national topographic dataset with high positional accuracy suitable for hydrological modelling.
Altitude	Elevation layer	Derived from DEM	Raster	10 m	Derived	Generated using ArcGIS Spatial Analyst	Directly extracted from the DEM, ensuring consistency with elevation data.
Slope	Slope gradient	Derived from DEM	Raster	10 m	Derived	Generated using ArcGIS Spatial Analyst	Standard terrain derivative widely used in flood susceptibility studies.
Flow accumulation	Flow accumulation raster	Derived from DEM	Raster	10 m	Derived	Generated using ArcGIS Hydrology tools	Computed using standard flow direction and accumulation algorithms.
Stream proximity	Euclidean distance to the drainage network	Derived from DEM	Raster	10 m	Derived	Generated using ArcGIS Euclidean Distance tool	Accurately represents the influence of the hydrographic network.
Lithology	Geological formations	BNEDER	Vector	1:50,000	Official administrative dataset	Digitized from the official geological map	Official geological information provided by the National Office for Rural Development (BNEDER).
Land use / Land cover	Land-use classification from Landsat 8 OLI	USGS EarthExplorer	Raster	30 m	2025	Image classification and preprocessing	Landsat 8 imagery is radiometrically and geometrically corrected and internationally recognized for land-cover mapping.
Precipitation	Rainfall interpolation from 13 meteorological stations and WorldClim	Meteorological stations + WorldClim v2.1	Raster	~1 km	2025	Spatial interpolation	Combines local rainfall observations with the validated WorldClim climatic database.
Flood Inventory	Historical flood occurrence database	Civil protection authority	Vector (Points)	Point observations	2011–2024	Georeferenced and field verified	Official flood inventory validated through field investigations and historical records.

reported flood locations. These surveys aimed to verify the spatial accuracy of the historical records and to identify physical evidence associated with previous flooding. Field observations revealed several hydraulic deficiencies that contribute to flood occurrence, including undersized culverts, obstruction of drainage structures by solid waste, sediment accumulation within drainage channels, and insufficient maintenance of hydraulic infrastructures, as illustrated in Figure 4. These observations provided direct physical evidence supporting the historical records and confirmed the susceptibility of the documented locations to flooding.

The field surveys further showed that these hydraulic deficiencies are predominantly concentrated in areas located close to the hydrographic network and within the downstream sections of the watershed, where floodwaters frequently overflow during intense rainfall events. The spatial agreement between the observed field conditions and the areas identified as High and Very High flood vulnerability by the GIS–AHP model provides additional confidence in the reliability of the historical flood inventory. This consistency between historical records, field observations, and model predictions confirms that the selected flood occurrence points adequately represent the spatial distribution of past flooding within the watershed.

To establish a balanced validation dataset, 180 non-flood points were also generated. These points were randomly distributed throughout the watershed in locations where no historical flood occurrence has been reported. Their selection was supported by field observations and high-resolution satellite imagery, which confirmed the absence of visible flood evidence or hydraulic dysfunctions. River channels, floodplains, and areas immediately surrounding documented flood locations were excluded from the sampling process to minimize classification uncertainty and avoid potential spatial bias. Consequently, the selected non-flood points represent areas considered free from historical flooding based on the available documentary records and field observations.

The final inventory, consisting of 360 reference locations (180 flood and 180 non-flood points), was subsequently used as an independent dataset to evaluate the predictive capability of the GIS–AHP flood vulnerability model through the success rate curve (SRC), area under the curve (AUC), and success curve area ratio (SCAR).

Figure 4 illustrates representative hydraulic deficiencies observed at several documented flood locations: (a) undersized culvert partially obstructed by solid waste; (b) sediment accumulation reducing channel conveyance capacity; (c) multiple culverts with limited hydraulic capacity; (d) deteriorated drainage section restricting water flow; (e) bridge crossing with insufficient hydraulic opening; and (f) poorly maintained drainage channel partially obstructed by vegetation and sediment. These field observations were used to verify historical flood locations and support the reliability of the flood inventory.

METHODOLOGY

Multi-criteria decision analysis

Flood vulnerability is controlled by the interaction of several topographic, geological, hydrological, and land-use factors. Because these variables contribute differently to flood generation, a MCDA approach was adopted to integrate them within a GIS. Among the available MCDA techniques, the AHP proposed by Saaty (1980) was selected owing to its ability to combine expert knowledge with quantitative analysis through pairwise comparisons.

The overall methodology consisted of four successive steps: (i) selection of the flood-conditioning factors, (ii) pairwise comparison and weighting of the selected criteria using the AHP approach, (iii) consistency verification of the comparison matrix, and (iv) weighted overlay analysis in GIS to produce the final flood vulnerability map.

Analytical hierarchy process

The AHP is a structured multicriteria decision-making technique that determines the relative importance of several criteria through pairwise comparisons (Saaty, 1980; Saaty, 1990). In this study, seven flood-conditioning factors were considered: altitude, slope, lithology, land use, precipitation, stream proximity, and flow accumulation.

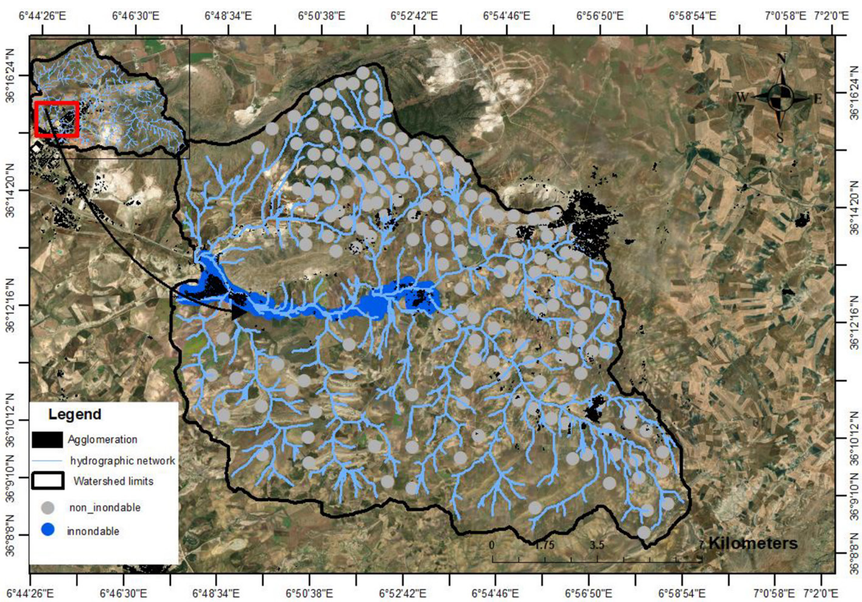

Figure 3. Spatial distribution of the historical flood inventory database used for model validation, showing the 180 flood occurrence points and the 180 non-flood points within the Oued Bounouara watershed

Figure 4. Field investigations conducted to verify the historical flood inventory database in the Oued Bounouara watershed

Each criterion was compared with every other criterion using Saaty's nine-point fundamental scale, where values range from 1 (equal importance) to 9 (extreme importance). These comparisons produced a reciprocal 7 × 7 pairwise comparison matrix, from which the normalized priority weights were derived using the principal eigenvector method.

To verify the logical consistency of the expert judgments, the pairwise comparison matrix was evaluated using the maximum eigenvalue (λmax), the consistency index (CI), and the consistency ratio (CR) according to Saaty (1980). The maximum eigenvalue was calculated as:

$$\lambda max = \frac{\sum \frac{(Aw)i}{wi}}{n} \quad (1)$$

where: *A* represents the pairwise comparison matrix, *w* is the normalized weight vector, and *n* is the number of criteria.

The Consistency Index was then computed as:

$$CI = \frac{\lambda max - n}{n-1} \quad (2)$$

The Consistency Ratio was calculated using:

$$CR = \frac{CI}{RI} \quad (3)$$

where: *RI* is the Random Index proposed by Saaty. For seven criteria (n = 7), *RI* = 1.32.

The consistency analysis yielded the following values:

Number of criteria (n) – value 7, maximum eigenvalue (λmax) – value 7.467, consistency index (CI) – value 0.078, random index (RI) – value 1.32, consistency ratio (CR) – value 0.059.

Since the calculated CR (0.059) is lower than the threshold value of 0.10, the pairwise comparison matrix is considered logically consistent, indicating that the expert judgments are reliable and suitable for deriving the thematic weights used in the flood vulnerability assessment.

Weighting of flood vulnerability factors

The pairwise comparison procedure produced the normalized weights presented in Table 2.

The results indicate that altitude (35.30%) is the most influential factor controlling flood vulnerability within the Oued Bounouara watershed, followed by slope (24.06%) and stream proximity (15.59%). Together, these three criteria account for approximately 75% of the total weight, highlighting the dominant role of topographic and hydrological conditions in controlling runoff generation and flood propagation.

Lithology (10.40%) and land use (6.06%) exhibit moderate influence by affecting infiltration capacity and surface runoff characteristics. In contrast, precipitation (5.54%) and flow accumulation (2.74%) received comparatively lower weights, reflecting the predominance of local topographic controls over rainfall variability within the study area.

Overall, the obtained weighting distribution is consistent with previous flood vulnerability studies conducted in Mediterranean environments, where elevation, slope, and proximity to drainage networks are generally recognized as the principal factors governing flood susceptibility.

GIS-based flood vulnerability mapping

Following the determination of the thematic weights, all standardized raster layers were integrated in ArcGIS 10.8 using the Weighted Overlay tool. Before the overlay analysis, all datasets were projected into the same coordinate reference system, clipped to the Oued Bounouara watershed boundary, resampled to a common spatial resolution of 10 m where appropriate, and standardized according to the predefined rating classes. The flood vulnerability index (FVI) was then calculated as:

$$\text{FVI}= \sum_{i=1}^{n}(\text{Wi} \times \text{Xi}) \quad (4)$$

where: *Wi* is the normalized weight assigned to criterion *i*; *Xi* is the standardized raster value of criterion *i*.

The resulting flood vulnerability index was subsequently classified into five categories using the Natural breaks (Jenks) classification method:

- Very low
- Low
- Moderate
- High
- Very high

The resulting flood vulnerability map constitutes the basis for the validation and performance assessment presented in the following section. The successful application of the GIS–AHP framework in this study is consistent with previous research demonstrating its effectiveness for flood hazard and vulnerability assessment due to its simplicity, transparency, and capacity to integrate multiple conditioning factors within a GIS environment (Taibi et al., 2024).

Reproducibility of the GIS–AHP framework

To ensure the reproducibility and transparency of the proposed GIS–AHP methodology, all analytical procedures adopted in this study are fully documented. The complete AHP pairwise comparison matrix, the normalized criterion weights, and the consistency assessment, including the λmax, CI, RI, and CR, are reported in the manuscript. The obtained (CR = 0.059) is below the

Table 2. Pairwise comparison matrix and normalized weights of the flood vulnerability factors

Parameter	Slope	Lithology	Land use	Precipitation	Stream proximity	Altitude	Flow accumulation
Slope	1	3	5	4	3	1/2	5
Lithology	1/3	1	2	3	1/2	1/4	5
Land use	1/5	1/2	1	2	1/4	1/6	3
precipitation	1/4	1/3	1/2	1	1/3	1/5	4
Stream proximity	1/3	2	4	3	1	1/3	7
Altitude	2	4	6	5	3	1	9
Flow accumulation	1/5	1/5	1/3	1/4	1/7	1/9	1
Weight	24.06	10.4	6.06	5.54	15.59	35.30	2.74

recommended threshold of 0.10, confirming the logical consistency of the pairwise comparisons and the reliability of the derived criterion weights.

The flood vulnerability assessment was implemented in ArcGIS 10.8 using a Weighted Overlay approach based on seven flood-conditioning factors: altitude, slope, lithology, land use, precipitation, stream proximity, and flow accumulation. Prior to the weighted overlay analysis, all spatial datasets were projected into a common coordinate reference system, clipped to the Oued Bounouara watershed boundary, resampled to a common spatial resolution of 10 m where appropriate, and standardized according to the rating scheme defined for each thematic layer.

The metadata of all input datasets, including their source, acquisition year, spatial resolution, quality, and reliability, are summarized in Table 1. Four thematic layers (altitude, slope, flow accumulation, and stream proximity) were derived from the 10 m digital elevation model using the ArcGIS Spatial Analyst and Hydrology toolsets, whereas the remaining datasets were obtained from official governmental institutions and internationally recognized databases. The complete methodological workflow, together with the data processing sequence and the weighted overlay equation used to compute the flood vulnerability index (FVI), is provided to facilitate the independent reproduction of the proposed methodology using equivalent datasets and GIS software.

FLOOD VULNERABILITY ASSESSMENT OF THE OUED BOUNOUARA WATERSHED

Flood conditioning factors

The flood vulnerability assessment was based on seven environmental and hydrological conditioning factors: land use, precipitation, lithology, slope, stream proximity, altitude, and flow accumulation. These factors were prepared as raster layers in a GIS environment and standardized prior to the AHP weighting procedure. Their spatial distributions are presented in Figure 5, illustrates the main physical characteristics controlling flood susceptibility within the Oued Bounouara watershed. Land use is dominated by agricultural areas in the central and southern parts of the watershed, whereas urbanized areas are mainly concentrated in the western sector. Agricultural land and bare soils generally reduce infiltration capacity and promote surface runoff during intense rainfall events.

The precipitation map shows a north–south gradient ranging from approximately 76 mm to 115 mm, indicating greater rainfall inputs in the northern sector of the watershed. Although precipitation contributes to runoff generation, its spatial variability is less influential than the topographic controls identified through the AHP weighting procedure.

The lithological map highlights the predominance of clayey sandstones, limestones, and marls, whose contrasting permeability significantly affects infiltration and runoff processes. Low-permeability formations are mainly associated with increased surface runoff and consequently higher flood susceptibility.

Topographic conditions exhibit strong spatial variability across the watershed. Steep slopes and higher elevations dominate the northern and western sectors, whereas lower elevations and gentler slopes characterize the downstream areas. In addition, the distance-to-stream map reveals that areas located close to the hydrographic network are more directly exposed to flood overflow because of their hydraulic connectivity.

Overall, the combined spatial distribution of these seven conditioning factors provides the basis for the GIS–AHP flood vulnerability assessment and reflects the complex interaction between topography, geology, hydrology, and land use within the Oued Bounouara watershed.

Flood vulnerability map

The GIS–AHP analysis produced the flood vulnerability map shown in Figure 6, which classifies the watershed into five vulnerability levels: Very Low, Low, Moderate, High, and Very High.

The quantitative analysis indicates that approximately 15% of the watershed is classified as Very Low vulnerability, 26% as Low, 25% as Moderate, 19% as High, and 15% as Very High vulnerability. Consequently, nearly 34% of the watershed (61.54 km²) belongs to the High and Very High vulnerability classes, representing the areas most susceptible to flooding.

Spatially, the highest vulnerability is concentrated in the western and downstream sectors of the watershed, particularly along the main hydrographic network and within low-lying valley bottoms. These areas correspond to zones where runoff converges and floodwaters accumulate during

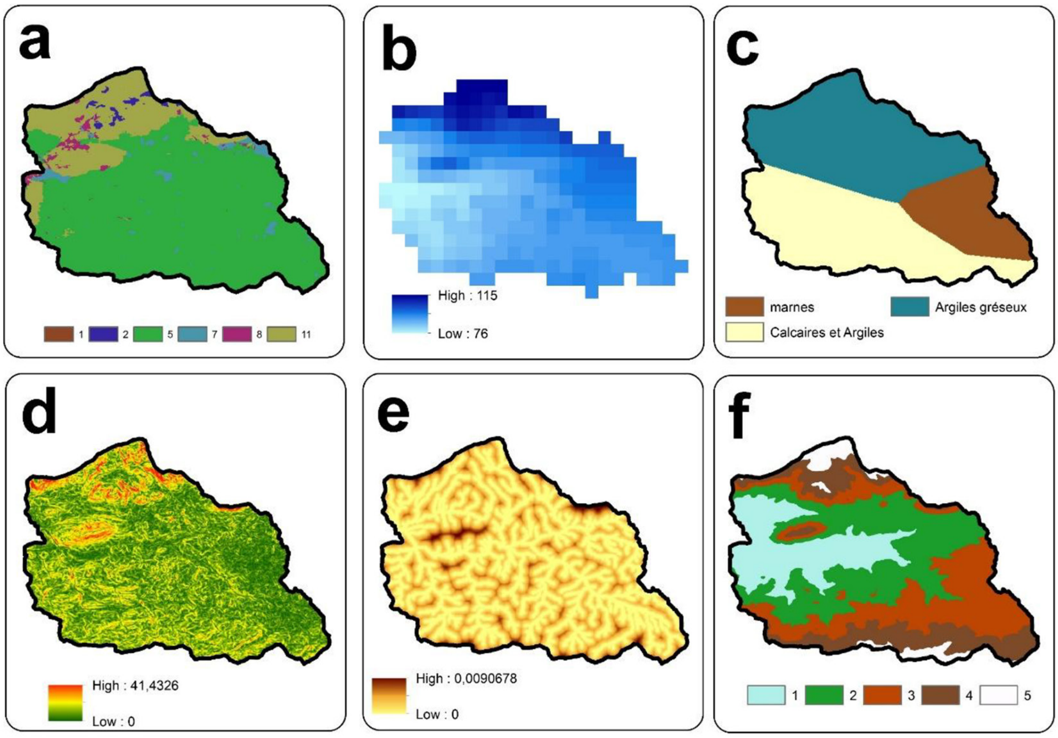

Figure 5. Spatial distribution of the seven flood-conditioning factors used in the GIS–AHP flood vulnerability assessment: (a) land use, (b) precipitation, (c) lithology, (d) slope, (e) stream proximity, (f) altitude, and (g) flow accumulation

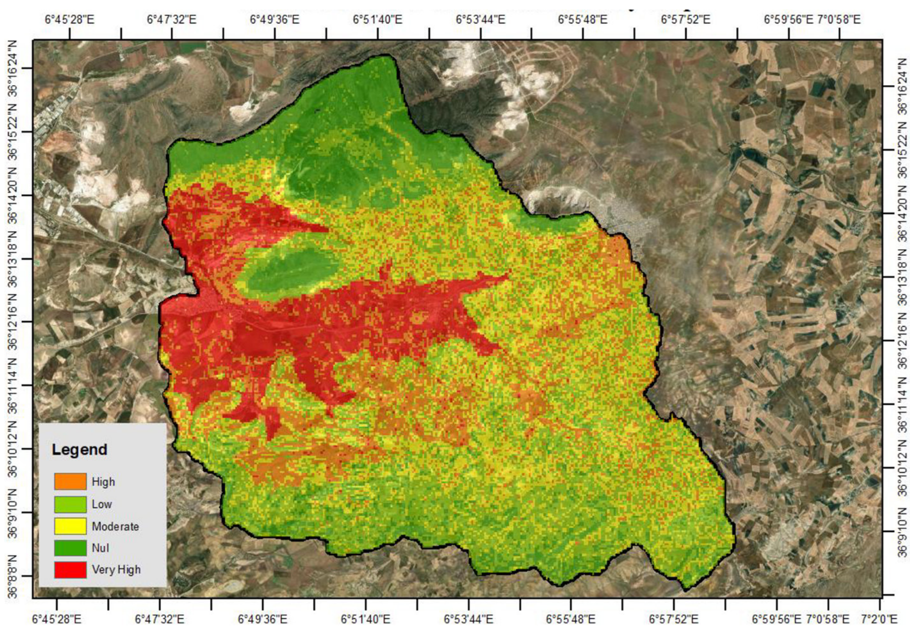

Figure 6. Flood Vulnerability map, watershed Bounouara

intense rainfall events. In contrast, the southern and southeastern sectors are predominantly classified as Low or Very Low vulnerability owing to their more favorable topographic and hydrological conditions.

The spatial distribution of flood vulnerability closely reflects the weighting results obtained through the AHP analysis. Altitude (35.30%) represents the most influential factor controlling flood vulnerability, followed by slope (24.06%) and stream proximity (15.59%). Together, these three criteria account for approximately 75% of the total weight, demonstrating that terrain morphology and hydrogeomorphological characteristics are the principal drivers of flood susceptibility within the watershed.

Lithology (10.40%) also contributes to flood generation by influencing infiltration capacity and runoff production, whereas land use (6.06%), precipitation (5.54%), and flow accumulation (2.74%) play comparatively smaller roles in the overall vulnerability assessment. Although these factors remain important, their lower weights indicate that local topographic conditions exert stronger control over flood occurrence in the Oued Bounouara watershed.

The predominance of topographic factors observed in this study is consistent with previous flood vulnerability investigations conducted in Mediterranean environments, where elevation, slope, and proximity to drainage networks are generally identified as the primary controls governing flood susceptibility (Okinomidis et al., 2015; Al-Abadi et al., 2017).

Overall, the resulting flood vulnerability map provides a realistic representation of the spatial distribution of flood-prone areas within the Oued Bounouara watershed. It constitutes the basis for the independent validation presented in the following section using the historical flood inventory, field verification, and quantitative performance indicators.

MODEL VALIDATION AND PERFORMANCE ASSESSMENT

Validation dataset

The predictive performance of the proposed GIS–AHP flood vulnerability model was assessed using an independent historical flood inventory database described in Section 2. The validation dataset consists of 180 documented flood occurrence points and 180 non-flood points, compiled from multiple reliable sources, including Civil Protection records, municipal archives, historical flood reports, and field surveys.

These reference data were not used during the AHP weighting procedure or during the development of the flood vulnerability model. Therefore, they provide an independent dataset for evaluating the spatial predictive capability and reliability of the proposed GIS–AHP approach.

The spatial distribution of the validation dataset is presented in Figure 5. Flood occurrence locations are mainly concentrated along the main river channel, floodplain areas, and downstream zones, where hydrological processes favor flood generation and propagation. In contrast, non-flood locations are distributed across areas where no historical flood events have been documented. The balanced distribution of the validation samples ensures a consistent comparison between flood-prone and non-flood-prone areas.

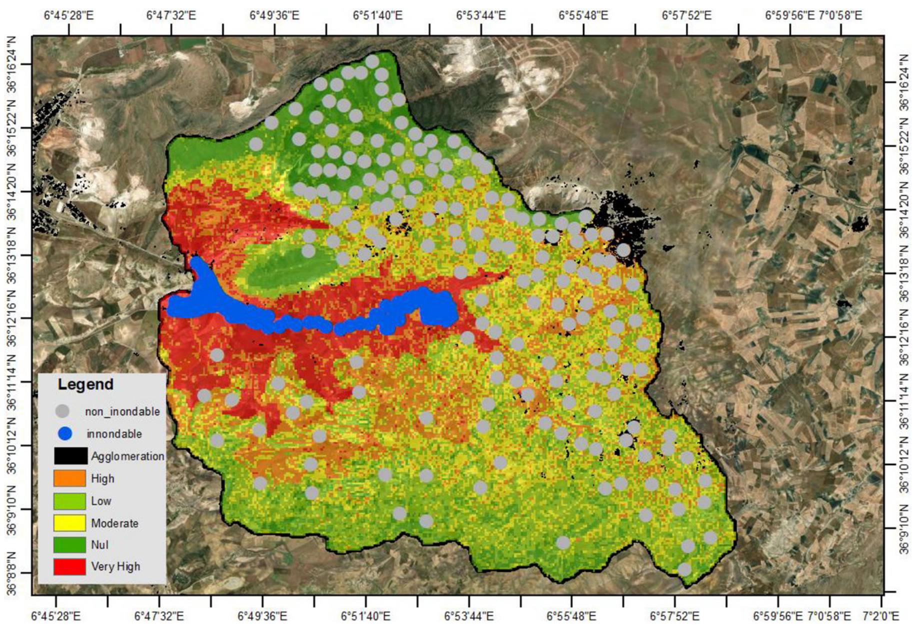

Figure 7. Validation vulnerability map, watershed Bounouara

Spatial validation of the flood vulerability map

The spatial relationship between the historical flood inventory and the GIS–AHP flood vulnerability map is illustrated in Figure 7. The validation was performed by overlaying an independent database of 360 reference points, comprising 180 documented flood occurrence points and 180 non-flood points, onto the final flood vulnerability map to evaluate the agreement between observed flood occurrences and the predicted vulnerability classes.

The results demonstrate a strong spatial correspondence between the model predictions and the historical flood inventory. All 180 documented flood occurrence points (100%) are located within the high and very high vulnerability classes, although these two classes collectively occupy only 34% of the watershed area (61.54 km² out of 181 km²). Specifically, 120 flood occurrence points (66.7%) fall within the very high vulnerability class, whereas the remaining 60 points (33.3%) are located in the high vulnerability class. This result does not imply perfect prediction; rather, it indicates that all documented historical flood events occurred within the two vulnerability classes identified by the model as the most susceptible to flooding.

Conversely, the majority of the 180 non-flood points are distributed within the moderate, low, and very low vulnerability classes, indicating good discrimination between flood-prone and relatively stable areas. The inclusion of non-flood reference points provides an independent evaluation of model performance and reduces the possibility of biased validation based solely on historical flood locations.

The observed spatial distribution confirms the capability of the GIS–AHP model to accurately identify areas exposed to flooding. Most flood occurrences are concentrated along the main river corridor and downstream floodplains, reflecting the combined influence of topographic and hydrological controls on flood generation. Among the conditioning factors, elevation, slope, flow accumulation, stream proximity, precipitation, land use, and lithology play complementary roles in explaining the spatial variability of flood vulnerability within the Oued Bounouara watershed. These findings are further supported by the quantitative validation metrics presented in the following section, including the success rate curve (AUC) and the success curve area ratio (SCAR), which independently confirm the predictive reliability of the proposed GIS–AHP model (Figure 8).

Success rate curve analysis

The predictive performance of the GIS–AHP flood vulnerability model was quantitatively evaluated using the success rate curve (SRC), which represents the relationship between the cumulative percentage of historical flood occurrences captured by the model and the cumulative percentage of watershed area ranked from the lowest to the highest flood vulnerability classes (Figure 9).

The obtained curve shows that 100% of historical flood occurrences are captured within only 34% of the watershed area, corresponding to the high and very high vulnerability classes. This result highlights the strong spatial concentration of historical flood events within areas identified as highly vulnerable and demonstrates the ability of the proposed GIS–AHP model to effectively prioritize flood-prone zones.

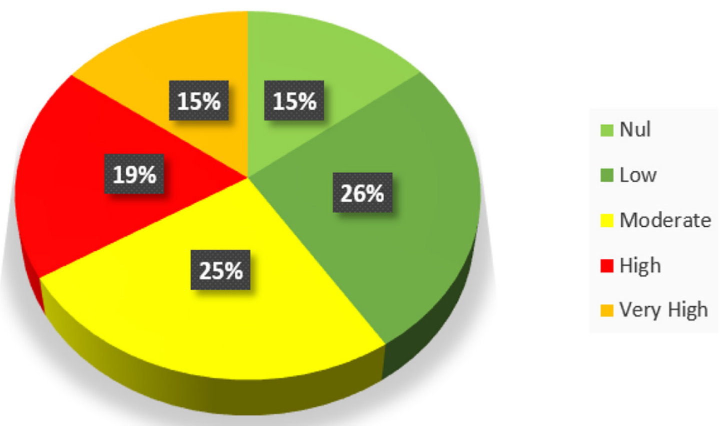

Figure 8. Distribution of flood vulnerability levels in the Bounouara Watershed

The area under the AUC was calculated using the trapezoidal integration method:

$$AUC=\sum \frac{(xi+1-xi)(yi+yi+1)}{2} \quad (5)$$

where: Xi represents the cumulative watershed area (%), yi represents the cumulative flood capture (%).

The calculated AUC value of 0.795 indicates a good discriminatory performance of the proposed GIS–AHP model according to the classification proposed by Hosmer and Lemeshow (2000). Values between 0.70 and 0.80 indicate acceptable to good discrimination, whereas values exceeding 0.80 are generally considered indicative of excellent predictive performance.

For comparison, a random prediction reference line (AUC = 0.50) was included in the SRC analysis. The difference between the observed curve and the random reference demonstrates the significant improvement achieved by the proposed GIS–AHP model in identifying areas with higher flood vulnerability.

The obtained AUC value is consistent with previous GIS-based flood vulnerability studies, confirming the effectiveness of the proposed methodology under semi-arid Mediterranean environmental conditions.

Success curve area ratio (SCAR)

To further evaluate the spatial efficiency of the GIS–AHP model, the SCAR was calculated as follows:

$$SCAR=\frac{Flood\ Capture\ Percentage}{Spatial\ Area\ \ Percentage} \quad (6)$$

$$SCAR = \frac{100}{34} = 2.94 \quad (7)$$

A SCAR value greater than one indicates that historical flood occurrences are concentrated within a relatively small proportion of the watershed classified as highly vulnerable. The obtained value (SCAR = 2.94) demonstrates the efficiency of the GIS–AHP model in concentrating observed flood events within the most vulnerable areas.

The high SCAR value obtained in this study is consistent with previous GIS-based flood mapping studies, where historical flood occurrences were found to be strongly clustered within zones characterized by high flood susceptibility (Rahmati et al., 2016).

Therefore, the SCAR analysis provides additional evidence that the proposed GIS–AHP framework successfully identifies spatial patterns of flood vulnerability and efficiently delineates priority areas for flood risk management.

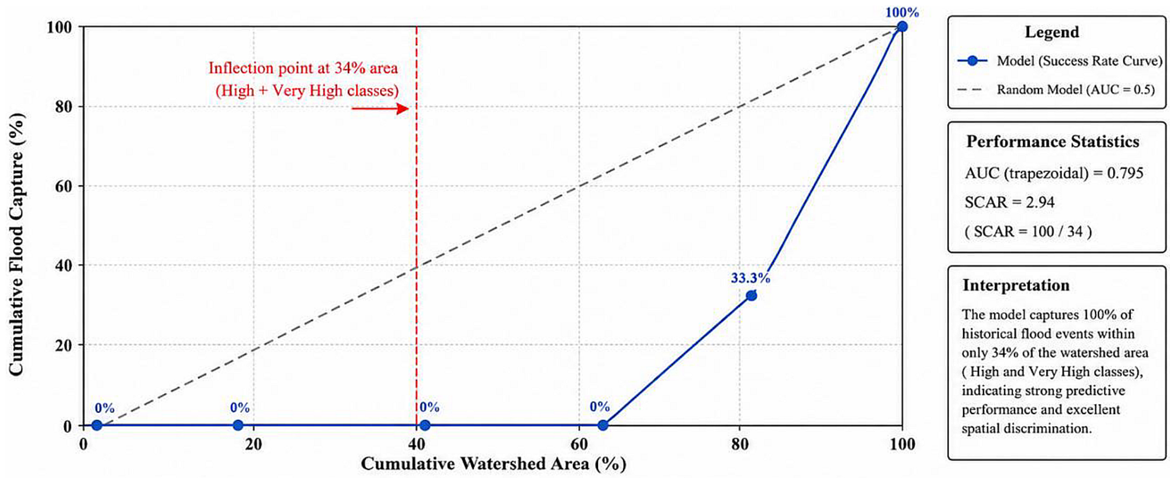

Vulnerability Class	Area (%)	Area (km²)	Flood Points (n = 180)	Flood Occurrence (%)	Cumulative Area (%)	Cumulative Flood Capture (%)
Very Low	15	27.15	0	0.0	15	0.0
Low	26	47.06	0	0.0	41	0.0
Moderate	25	45.25	0	0.0	66	0.0
High	15	27.15	60	33.3	81	33.3
Very High	19	34.39	120	66.7	100	100.0
Total	**100**	**181.00**	**180**	**100.0**	**100**	**100.0**

Notes:
- Flood inventory: 180 events (independent dataset)
- AUC computed using the trapezoidal integration method
- SCAR > 1 indicates strong spatial concentration of floods in high susceptibility zones

Figure 9. Success rate curve (cumulative flood capture vs cumulative area) for the GIS-AHP flood vulnerability model

Reliability assessment of the GIS–AHP model

The reliability of the proposed GIS–AHP flood vulnerability model is supported by several complementary validation procedures.

First, the pairwise comparison matrix satisfied Saaty's consistency criterion, with a CR lower than the recommended threshold of 0.10. This confirms the logical consistency of expert judgments and supports the reliability of the derived thematic weights.

Second, the historical flood inventory used for validation was compiled from multiple independent sources, including civil protection records, municipal archives, historical reports, satellite imagery, and field investigations. Since these reference data were not involved in the AHP weighting procedure or model construction, they provide an unbiased basis for evaluating the predictive performance of the proposed framework.

Finally, the strong spatial agreement between historical flood occurrences and predicted flood vulnerability classes (Figure 6), combined with the satisfactory AUC value (0.795) and the high SCAR value (2.94), confirms the robustness and predictive capability of the GIS–AHP model for flood vulnerability assessment in the Oued Bounouara watershed.

CONCLUSIONS

This study presents the first comprehensive flood vulnerability assessment of the Oued Bounouara watershed (northeastern Algeria) by integrating GIS and AHP within a transparent and reproducible spatial modelling framework. Although the GIS–AHP methodology is well established, its application to this previously unstudied peri-urban Mediterranean watershed provides new insights into the spatial distribution of flood vulnerability in an area characterized by recurrent flood events, rapid urban expansion, and increasing socio-environmental exposure.

The flood vulnerability map identified approximately 34% of the watershed area as belonging to the high and very high vulnerability classes, primarily concentrated along the main hydrographic network and downstream floodplain areas. These results demonstrate that flood vulnerability in the Oued Bounouara Watershed is mainly controlled by the combined influence of topographic and hydrological factors, particularly elevation, slope, flow accumulation, stream proximity, together with lithology, land use, and precipitation.

The reliability of the proposed model was assessed using an independent validation database composed of 180 documented flood occurrence points and 180 non-flood reference points, compiled from civil protection records, municipal archives, historical reports, satellite image interpretation, and field investigations. The validation results showed a strong spatial agreement between observed flood occurrences and the predicted vulnerability classes, with all documented flood events located within the high and very high vulnerability zones, although these classes represent only 34% of the watershed area. This result, together with the inclusion of non-flood reference points, confirms the strong discriminatory capability of the proposed model rather than implying perfect prediction.

Additional quantitative validation further demonstrated the robustness of the proposed methodology. The success rate curve produced an area under the curve (AUC) of 0.795, indicating good predictive performance, while the success curve area ratio (SCAR = 2.94) confirmed the strong concentration of historical flood events within highly vulnerable areas. Field investigations further supported these findings by identifying insufficient drainage capacity, sediment accumulation, obstructed hydraulic structures, and inadequate maintenance as major factors contributing to local flood occurrence.

Beyond its scientific contribution, the proposed flood vulnerability map constitutes an effective decision-support tool for flood risk management. The identified high-vulnerability areas should be prioritized for land-use regulation, drainage system improvement, hydraulic infrastructure rehabilitation, watershed management, and emergency planning. The generated spatial information can support local authorities in reducing flood impacts while promoting sustainable territorial planning and climate adaptation strategies.

Although the proposed framework produced reliable results, several limitations should be acknowledged. The AHP weighting procedure inevitably involves a degree of expert judgement, and the present assessment mainly considers the physical and environmental factors controlling flood vulnerability. Future studies should incorporate socioeconomic vulnerability indicators, higher-resolution topographic datasets, hydrodynamic modelling, climate change scenarios, and advanced machine-learning techniques to further improve flood prediction and risk assessment.

Overall, this study fills an important knowledge gap by providing the first GIS-based flood vulnerability assessment of the Oued Bounouara Watershed, a rapidly urbanizing peri-urban catchment that has received limited scientific attention despite its recurrent flood history. The integration of official governmental datasets, remote sensing products, historical flood inventories, and field observations within a reproducible GIS–AHP framework demonstrates that reliable flood vulnerability assessment can be achieved even in data-scarce environments. Consequently, the proposed methodology offers a robust and transferable framework that can readily be applied to other Mediterranean watersheds facing similar hydrological, environmental, and urbanization challenges.

The datasets used in this study originate from publicly available sources, official institutional databases, and datasets generated by the authors. Landsat 8 OLI imagery is publicly available through the USGS EarthExplorer platform, and climatic data are publicly accessible from the WorldClim database. These datasets can be obtained directly from their respective repositories.

The DEM was obtained from the National Institute of Geographic Information (Paris 12) and was used to derive the altitude, slope, flow accumulation, and stream proximity layers through ArcGIS spatial analysis. These derived layers, together with the flood susceptibility maps and the AHP weighting results, were generated by the authors during the course of this research.

The lithological map was obtained as an official administrative document from the National Office for Rural Development (BNEDER) and is not publicly distributed. The historical flood inventory used for model validation was provided by the civil protection authority and contains official records subject to institutional restrictions. The DEM, lithological data, and flood inventory may be made available by the corresponding author upon reasonable request and with permission from the respective data providers.

REFERENCES

1. Al-Abadi, A. M., Shahid, S., Al-Shaibani, S. (2017). Flood susceptibility mapping using analytical hierarchy process in Ain Tapra region, Iraq. *International Journal of Disaster Risk Reduction, 24*, 367–378. https://doi.org/10.1016/j.ijdrr.2017.06.007
2. Aktar, M., Shohani, K., Hasan, M., Hasan, M. (2021). Flood vulnerability assessment by flood vulnerability index (FVI) method: A study on Sirajganj Sadar Upazila. *International Journal of Disaster Risk Management*.
3. Arabameri, A., Pradhan, B., Rezaei, K., Yamani, M. (2021). Flood susceptibility mapping using ensemble of bivariate statistical models with GIS. *Natural Hazards, 105*(1), 893–920. https://doi.org/10.1007/s11069-020-04377-5
4. Azemeraw Wubalem, G. T., Dawit, Z., Getahun, B., Mekuria, T., Jothimani, M. (2020). Comparison of statistical and analytical hierarchy process methods on flood susceptibility mapping: A case study of Lake Tana sub-basin. *Open Geosciences*.
5. Benoudina, N. A., Djeghar, A., Grecu, F., Bouguerraa, A., Taibi, I. E. K. (2026). Flood risk assessment in a semi-arid Mediterranean basin using HEC-RAS hydraulic simulation: A case study of Oued Bounouara. *Environment Conservation Journal, 27*(1), 358–376. https://doi.org/10.36953/ECJ.34853175
6. Benoudina, N. A., Djeghar, A., Grecu, F., Bouguerraa, A., Taibi, I. E. K. (2026). Flood risk assessment in a semi-arid Mediterranean basin using HEC-RAS hydraulic simulation: A case study of Oued Bounouara. *Environment Conservation Journal, 27*(1), 360. https://doi.org/10.36953/ECJ.34853175
7. Benoudina, N. A., Djeghar, A., Grecu, F., Bouguerraa, A., Taibi, I. E. K. (2026). Flood risk assessment in a semi-arid Mediterranean basin using HEC-RAS hydraulic simulation: A case study of Oued Bounouara. *Environment Conservation Journal, 27*(1), 372. https://doi.org/10.36953/ECJ.34853175
8. Berger, C., Moser, M., Hofmeister, F. (2019). Spatial variability of precipitation and its impact on flood generation in Alpine catchments. *Journal of Hydrology, 578*, 124056. https://doi.org/10.1016/j.jhydrol.2019.124056
9. Boukhiar, F., Boutebba, H., Medjadj, T. (2024). L'évolution diachronique des interactions urbanisation-cours d'eau: Cas de la ville de Béjaïa. *Revue Roumaine de Géographie*.
10. Bourenane, H., Bouhadad, Y. (2020). Spatial analysis, assessment and mapping of flood hazards in the alluvial plains of Boumerzoug and Rhumel (Constantine, Algeria). *Bulletin of Engineering Geology and the Environment*.
11. Chen, W., Li, Y., Wang, E. (2019). Flood susceptibility assessment based on GIS and analytical hierarchy process in Yingtan, China. *Natural Hazards, 98*(2), 543–560. https://doi.org/10.1007/s11069-019-03694-6
12. Cowie, P., Atkinson, T., Bras, R. L. (2018). Lithological control on runoff generation in semi-arid catchments. *Hydrological Processes, 32*(15), 2367–2381. https://doi.org/10.1002/hyp.13189

13. Das, S. (2018). Geographic information system and AHP-based flood hazard zonation of Vaitarna basin, India. *Arabian Journal of Geosciences*.
14. Germanwatch. (2024). *Global Climate Risk Index 2024: Annual losses from extreme weather events*. Germanwatch Institute.
15. Ghosh, A., Kar, S. (2018). Application of analytical hierarchy process for flood risk assessment: A case study in Malda district of West Bengal, India. *Natural Hazards*.
16. Guellouh, S., Kalla, M., Ouahiba, L. (2023). A multi-criteria analytical hierarchy process (AHP) to flood vulnerability assessment in Batna watershed (Algeria). *Journal of Environmental Engineering and Geoscience, 29*(3), 245–262.
17. Hosmer, D. W., Lemeshow, S. (2000). Applied logistic regression (2nd ed.). John Wiley & Sons.
18. Kazakis, N., Kougias, I., Voutsinas, N., Voudouris, K. (2015). Application of the Analytical Hierarchy Process for flood susceptibility mapping in Greece. *Natural Hazards and Earth System Sciences, 15*(10), 2231–2243. https://doi.org/10.5194/nhess-15-2231-2015
19. Lu, H., Li, Y., Chen, S. (2019). Effect of bare soil exposure on surface runoff and erosion in agricultural watersheds. *Soil and Tillage Research, 194*, 104306. https://doi.org/10.1016/j.still.2019.104306
20. Meroti, A., Koutalakis, P., Zaimes, G. N. (2020). Slope gradient effects on runoff velocity and flood peak timing in Mediterranean watersheds. *Water, 12*(8), 2156. https://doi.org/10.3390/w12082156
21. Naghibi, S. A., Ahmadi, K., Daneshvar, M. R. M. (2020). GIS-based multi-criteria decision analysis for flood susceptibility mapping. *Environmental Earth Sciences, 79*(15), 1–18. https://doi.org/10.1007/s12665-020-09118-4
22. Okinomidis, D., Dimogianni, S., Kazakis, N., Voudouris, K. (2015). Flood hazard assessment using GIS and analytical hierarchy process: A case study of Greece. *Environmental Earth Sciences, 74*(4), 3345–3358. https://doi.org/10.1007/s12665-015-4530-6
23. Oussalah, A., Belhadj, M., Djema, K. (2023). Geographic and climatic characteristics of Constantine region: Implications for water resources. *North African Journal of Environmental Science*.
24. Pal, S. C., Chowdhuri, I., Chakrabortty, R. (2021). Impact of land use/land cover changes on flood risk in a tropical river basin. *Spatial Information Research, 29*(3), 389–404. https://doi.org/10.1007/s41324-020-00356-0
25. Pham, B. T., Prakash, I., Dou, J. (2020). Flood susceptibility modeling using machine learning ensembles. *Journal of Hydrology, 575*, 874–887. https://doi.org/10.1016/j.jhydrol.2019.05.085
26. Prosdocimi, M., Burgan, G., Tarolli, P. (2016). Agricultural land use and flood risk: A review. *Earth-Science Reviews, 162*, 194–212. https://doi.org/10.1016/j.earscirev.2016.09.004
27. Rahmati, O., Pourghasemi, H. R., Zeinivand, H. (2016). Flood susceptibility mapping using frequency ratio and weights-of-evidence models. *Geomatics, Natural Hazards and Risk, 7*(5), 1509–1538. https://doi.org/10.1080/19475705.2015.1045043
28. Rebouh, N., Tout, F., Dinar, H., Benzid, Y., Zouak, Z. (2024). Integrating multi-source geospatial data and AHP for flood assessment. *International Journal of Disaster Risk Management*.
29. Saaty, T. L. (1980). *The analytic hierarchy process: Planning, priority setting, resource allocation*. McGraw-Hill.
30. Tehrany, M. S., Pradhan, B., Mansor, S. (2019). Flood susceptibility assessment using GIS-based AHP and frequency ratio models. *International Journal of Disaster Risk Reduction, 38*, 101193. https://doi.org/10.1016/j.ijdrr.2019.101193
31. Tremlett, A. E., Lees, B. G., Evans, C. D. (2021). Topographic controls on flood susceptibility in upland catchments. *Hydrological Processes, 35*(3), e14089. https://doi.org/10.1002/hyp.14089
32. UNISDR. (2015). *Sendai Framework for Disaster Risk Reduction 2015–2030*. United Nations Office for Disaster Risk Reduction.
33. Vigiak, O., Grizzetti, B., Nunes, J. P. (2012). Effectiveness of forested buffer zones in reducing flood risk. *Environmental Management, 50*(4), 635–651. https://doi.org/10.1007/s00267-012-9898-7
34. Ziadi, S., Keraghel, M. (2024). Flooding vulnerability in Algiers (Algeria): An analytic hierarchy process. *Natural Hazards*.